J. Fluid Mech. (1986), *vol.* 167, *pp.* 31–48
Printed in Great Britain

Boundary-layer separation of a two-layer rotating flow on a β-plane

By LEE-OR MERKINE
Department of Mathematics, Technion-Israel Institute of Technology, Haifa 32000, Israel

AND LEONID BREVDO
Geophysical Fluid Dynamics Laboratory/NOAA, Princeton University, Princeton, NJ 08540, USA

(Received 3 January 1985 and in revised form 29 November 1985)

The problem of quasi-geostrophic two-layer flow past a vertical cylinder on a β-plane is investigated analytically and numerically. Two parameter regimes are considered: (i) $0 \leqslant E^{\frac{1}{2}}/\epsilon \leqslant \infty$ and $\beta = O(1)$; (ii) $E^{\frac{1}{2}}/\epsilon \gg 1$ and $\beta\epsilon/E^{\frac{1}{2}} = O(1)$. ϵ is the Rossby number, E is the Ekman number and β is the beta parameter. In the first parameter regime the nonlinear interior and boundary-layer equations are integrated to determine if and when the wall shear stress vanishes so that an estimate of the condition for separation in the classical sense can be obtained. The results seem to explain the enhancement/suppression of separation in retrograde/prograde flows and the east–west asymmetry observed in the experiments of Boyer & Davies (1982). In the second parameter regime the analysis is linear and the vorticity balance is dominated by the β-effect and Ekman suction. When the flow at infinity is vertically sheared, two large standing interior eddies can be generated next to the cylinder. Only the interior solutions are given in (ii) since the boundary-layer flow is irrelevant to the large-scale behaviour.

1. Introduction

The problem of flow separation is a classical one in fluid mechanics but in the context of rotating fluids it started to attract interest only recently with the pioneering experimental work of Boyer (1970). Slightly viscous homogeneous flow was forced past a circular cylinder extending throughout the depth of the fluid. The axis of the cylinder was parallel to the constant rotation vector. The results of the experiments showed that separation was inhibited in the limit of vanishing nonlinear effects but it occurred for small-but-finite Rossby numbers. The theoretical studies of Walker & Stewartson (1972) and Merkine & Solan (1979) showed that the parameter controlling separation is proportional to the ratio of the Rossby number ϵ to the square root of the Ekman number E, and that separation is inhibited whenever the dissipation of vorticity induced by Ekman suction is dominant. The same conclusion was reached by Page (1982) when he considered flow separation in a rotating annulus with shallow topography.

Large-scale geophysical flows are typified by the existence of the dynamically important Rossby waves. These waves are non-isotropic, owing their existence to the variation of the Coriolis parameter with latitude. An important consequence of the non-isotropy is that the east–west symmetry enjoyed by the constant-Coriolis-parameter dynamics is broken. (Constant-Coriolis-parameter dynamics is referred to as the f-plane model. In the β-plane model the Coriolis parameter is allowed to vary linearly with latitude; all other effects of the Earth's sphericity are ignored. β-plane dynamics is often simulated in the laboratory by varying linearly in one horizontal direction the distance between the top and bottom bounding surfaces.) Thus it is expected that the dynamics of flow separation on a β-plane will be different from that on an f-plane.

White (1971) reported on an experimental study of a slightly viscous homogeneous prograde (eastward) flow past a circular cylinder on a β-plane and obtained qualitative agreement with theoretical results based on inviscid considerations. In White's study Ekman suction was of secondary importance, suggesting that the β-effect was responsible for inhibiting separation. Merkine (1980) studied the influence of a β-plane, measured by the non-dimensional parameter β, on the separation problem for White's parameter regime, namely $\beta = O(1)$ and negligible Ekman suction. The results show that β inhibits separation in prograde flows but exerts no influence on the boundary-layer dynamics in retrograde (westward) flows in qualitative agreement with White's experiment and also with the early experiments of the 1950s using spherical shells (see Merkine 1980 for discussion). Recently Boyer & Davies (1982) conducted a very careful and extensive experimental study of flow past a circular cylinder on a β-plane using a rotating channel with sloping top and bottom surfaces. They considered the parameter regime $\beta = O(1)$ and $\epsilon = O(E^{\frac{1}{2}})$ and found that β inhibits separation in prograde flows but enhances it in retrograde flows. The experimental study showed also that the downstream flows developed asymmetry with respect to the mainstream direction. An explanation for this asymmetry, which appeared also in Boyer's (1970) earlier experiments, was suggested by Merkine & Solan (1979). It is based on incorporating into the analysis higher-order Rossby-number effects.

The dynamics of large-scale geophysical flows is stratified to the extent that baroclinicity is as important as rotation. Hence, it is of interest to study the separation problem of rotating stratified flows with possible application to flows around island-like objects. Hogg (1972) studied rotating stratified inviscid flow past a tall topographic feature. The inclusion of frictional effects goes one step further. A good review of the influence of orography on planetary flows is given by Hogg (1980). The physically realizable two-layer model provides us with the simplest way of incorporating stratification into the dynamics. This approach was taken recently by Brevdo & Merkine (1985) who considered the f-plane dynamics. The linear dynamics for a continuously stratified fluid was investigated by Merkine (1985). These two studies demonstrate that on-coming flows that are of one sign but possess vertical shear can induce backflow regions next to the cylinder without separation ever taking place. The physical explanation for this surprising phenomenon differs from the two-layer model to the continuously stratified model. However, from a mathematical point of view this result emerges from the fact that the linear dynamics of slightly viscous rotating systems is spatially uniformly valid. Thus, the existence of backflow regions predicted by linear theory cannot be eliminated when small nonlinear effects are introduced. In this paper we study the problem of flow separation in the context of the two-layer model on a β-plane. We hope that the results obtained will provide the necessary impetus for new laboratory experiments.

The main conclusion of the experiments of Boyer & Davies (1982), namely that β inhibits separation in prograde flows but enhances it in retrograde flows, is based on estimating the size of the eddies induced by separation. No boundary-layer measurements were made, presumably because of the technical difficulties encountered in performing such measurements in rotating systems. Our analysis studies the boundary-layer structure and terminates at the point where the classical boundary-layer approximation breaks down, and the original outer solution is consequently modified. When this occurs, classical boundary-layer theory suggests that the wall shear stress vanishes in a singular manner as shown by Goldstein (1948). The phenomenon of separation refers to the detachment of the boundary layer from the wall which is accompanied by a region of reversed flow downstream of the separation point (Rosenhead 1963). Experience shows that the collapse of the classical boundary-layer theory usually heralds the onset of separation and the point of vanishing shear stress is used to estimate the separation point. When the latter moves upstream from the rear stagnation point the size of the eddies increases. It is in this sense that we can relate our results to the measurements of Boyer & Davies (1982) and find the comparison harmonious.

The collapse of classical boundary-layer theory does not necessarily signal the collapse of the boundary-layer approach. The triple-deck theory, an excellent review of which is given by Smith (1982), shows instances where it is possible to reformulate the boundary-layer problem in a way which allows determination of the boundary-layer structure as it detaches from the wall. This is not a simple matter, in particular for our coupled nonlinear boundary-layer equations, and no attempt is made here to apply the new strategy to the detached portion of the boundary layer. It is desirable that such a study should be carried out at a later time†.

2. The model

The model discussed in this section incorporates the β-effect into the model discussed by Brevdo & Merkine (1985). We consider a slightly viscous, quasi-geostrophic flow consisting of two layers of homogeneous, immiscible fluid confined vertically by rigid horizontal boundaries. The fluid density of the upper layer is slightly less than that of the lower layer so that the Boussinesq approximation is applicable. The system is on a β-plane, namely it rotates about the vertical z-axis with an angular velocity $\mathbf{\Omega}$ which is a linear function of the y-coordinate or equivalently the meridional direction of geophysical flows. Centrifugal effects are assumed negligible so that in the absence of motion the fluid interface is approximately level, the depths of the upper and lower layer are H_1 and H_2 respectively. A steady flow, not restricted horizontally, is forced past a vertical circular cylinder which extends throughout the depth of the fluid. At large distances from the cylinder the flow is unidirectional and along the x-axis. It is sheared vertically but not horizontally. Consistent with the quasi-geostrophic formalism, viscous effects are confined to thin boundary layers which are adjacent to the rigid horizontal surfaces and the interface and extend vertically along the cylinder.

We use the indices $n = 1, 2$ to denote properties of the upper and lower layers respectively. Then ν_n is the kinematic viscosity, U_n^* is the magnitude of the dimensional velocity at infinity and $g(\rho_2-\rho_1)/\rho_2$ is the reduced gravity. The gravitational acceleration is denoted by g and ρ_n is the density, L is the radius of the cylinder and $f = 2\Omega$ is the Coriolis parameter whose value and gradient at the reference latitude $y = 0$ are given by f_0 and β^1 respectively. Let $U^* = \frac{1}{2}(U_1^* + U_2^*)$ be

† We are grateful to one of the referees for bringing up this point.

the characteristic velocity of the horizontal motion and L the characteristic length. It follows that the dynamics of the problem are controlled by the following 6 non-dimensional parameters:

$$\epsilon = \frac{U^*}{f_0 L} \quad \text{the Rossby number,}$$

$$E_n = \frac{\nu_n}{f_0 H_n^2} \quad \text{the Ekman number,}$$

$$\delta_n = \frac{H_n}{L} \quad \text{the aspect ratio,}$$

$$F_n = \frac{L^2 f_0^2}{H_n g(\rho_2 - \rho_1)/\rho_2} \quad \text{the Froude number,}$$

$$\chi = \left(\frac{\nu_2}{\nu_1}\right)^{\frac{1}{2}} \quad \text{the viscosity ratio,}$$

$$\beta = \beta^1 L^2 / U^* \quad \text{the } \beta \text{ parameter.}$$

The parameter constraints imposed on the quasi-geostrophic motion are

$$\epsilon \ll 1, \quad E_n \ll 1, \quad \delta_n = O(1), \quad F_n = O(1), \quad \beta = O(1).$$

Here the constraints on δ_n, F_n and β are understood in the limit of $\epsilon \to 0$, $E_n \to 0$. No constraint is imposed on χ.

Away from thin viscous boundary layers of $O(E^{\frac{1}{2}})$ existing along the horizontal surfaces and the interface and of $O(E^{\frac{1}{3}})$ along the vertical cylinder the quasi-geostrophic dynamics prevail and they are determined by the following two equations governing the geostrophic pressure P_n.†

$$\left.\begin{aligned} J(P_1, Q_1) &= (E_1^{\frac{1}{2}}/2^{\frac{1}{2}}\epsilon)\left[-\nabla^2 P_1 + \frac{\chi}{\chi+1}(\nabla^2 P_2 - \nabla^2 P_1)\right] + (E_1 \delta_1^2/\epsilon)\nabla^4 P_1, \\ J(P_2, Q_2) &= (E_2^{\frac{1}{2}}/2^{\frac{1}{2}}\epsilon)\left[-\nabla^2 P_2 + \frac{1}{\chi+1}(\nabla^2 P_1 - \nabla^2 P_2)\right] + (E_2 \delta_2^2/\epsilon)\nabla^4 P_2. \end{aligned}\right\} \tag{2.1}$$

Q_n is the potential vorticity defined as

$$Q_n = \nabla^2 P_n + (-1)^n F_n (P_1 - P_2) + \beta y. \tag{2.2}$$

$J(P_n, Q_n)$ is the Jacobian of P_n and Q_n. Using a polar coordinate system for the horizontal motion with origin at the centre of the circular cross-section of the cylinder we have

$$J(P_n, Q_n) = \left(-\frac{1}{r}\frac{\partial P_n}{\partial \theta}\frac{\partial}{\partial r} + \frac{\partial P_n}{\partial r}\frac{1}{r}\frac{\partial}{\partial \theta}\right) Q_n. \tag{2.3}$$

Since the geostrophic pressure is constant along streamlines of the geostrophic motion the radial and tangential components of this lowest-order motion are given by

$$u_n = -\frac{1}{r}\frac{\partial P_n}{\partial \theta}, \quad v_n = \frac{\partial P_n}{\partial r} \tag{2.4}$$

respectively. It follows that $\nabla^2 P_n$ is the relative vorticity of the geostrophic motion.

† These equations are derived using ϵ as the expansion parameter. The above constraints imply that the displacement of the interface and the β-effect contribute to the dynamics at $O(\epsilon)$.

Equations (2.1) for the f-plane appear in Hart (1972). Their derivation is now standard and is given by Pedlosky (1979) for the case of an inviscid interface. Equations (2.1) state that following the geostrophic motion the geostrophic potential vorticity in each layer is changed as a result of vortex stretching and diffusion of vorticity. The vortex stretching is a consequence of the secondary circulation induced by the $O(E^{\frac{1}{2}})$ linear Ekman layers along the rigid horizontal surfaces and along the interface. Nonlinear effects in the Ekman layers can be ignored as long as $E = o(E^{\frac{1}{4}})$.

The first term in the square brackets on the right-hand side of (2.1) represents the spin-down effect induced by the Ekman layers along the rigid horizontal surfaces. The second term in these square brackets represents the spin-up of one layer by the other one as a consequence of a possible vorticity difference that might exist between the two layers. The last term on the right-hand side of (2.1) represents the mechanism of vorticity diffusion. Finally, we observe that relative vorticity can also be induced by the gradient of the planetary vorticity through meridional motions and by the motion of the interface whose deviation from a state of relative rest is given non-dimensionally by $P_2 - P_1$.

The Ekman layers whose effect on the quasi-geostrophic dynamics has been discussed above provide the transition region which adjusts the height-independent geostrophic motion of each layer to the no-slip condition at the horizontal surfaces and provide continuity of velocity and stress along the interface separating the two layers. The situation along the vertical wall of the cylinder is more complex and it is worthwhile recapitulating the results derived for homogeneous fluids. When $\epsilon \ll E^{\frac{1}{2}} \ll 1$ and $\beta = O(1)$ the advection terms in the vorticity balance can be ignored and the vertical boundary layer splits into two layers of thickness $O(E^{\frac{1}{4}})$ and $O(E^{\frac{1}{3}})$. Of these two the $E^{\frac{1}{4}}$ layer is thicker but both layers are wider than the $O(E^{\frac{1}{2}})$ Ekman layers (Greenspan 1968). The linear theory for a flow past a circular cylinder on an f-plane was discussed first by Barcilon (1970) and improved by Walker & Stewartson (1972). The essence of the analysis is that the $E^{\frac{1}{4}}$ layer adjusts the $O(1)$ interior geostrophic flow to the no-slip wall condition while the $E^{\frac{1}{3}}$ layer adjusts the lowest-order vertical velocity, which is $O(E^{\frac{1}{4}})$ in the vertical boundary layer, to the no-slip wall condition. It also follows that the $E^{\frac{1}{4}}$ layer is in geostrophic balance and hence merges smoothly with the interior geostrophic flow. The structure of the inner $E^{\frac{1}{3}}$ layer is height dependent and thus cannot satisfy the Taylor–Proudman theorem. Formally, nonlinear effects become important when $\epsilon = O(E^{\frac{1}{2}})$, a case treated also by Walker & Stewartson (1972) for the f-plane geometry. The vertical boundary layer still consists of two layers of widths $E^{\frac{1}{4}}$ and $E^{\frac{1}{3}}$. The outer $E^{\frac{1}{4}}$ layer becomes nonlinear but retains its geostrophy. The $E^{\frac{1}{3}}$ layer is still linear and so are the Ekman layers. As long as $\beta = O(1)$, the β-effect does not appear explicitly in the lowest-order boundary-layer equations.

Thus, when $\epsilon = O(E^{\frac{1}{2}})$ and $\epsilon \rightarrow 0$ the quasi-geostrophic barotropic vorticity equation with horizontal diffusion and a linear Ekman suction condition provides a uniformly valid representation of the dynamics of the geostrophic motion all the way to the vertical wall and the no-slip conditions along the cylinder can be expressed to lowest order in terms of the geostrophic velocity. The experimental results of Boyer (1970) show that as ϵ increases the flow field develops left–right asymmetry facing the downstream direction. Quasi-geostrophic formalism is not capable of explaining this effect and a different approach is necessary as demonstrated by Merkine & Solan (1979) for the f-plane case.

Returning to the baroclinic problem at hand we are led to the possible conclusion that since each layer is of constant density, the vertical boundary layer along the cylinder should split into a quasi-geostrophic $E^{\frac{1}{4}}$ layer and a non-geostrophic $E^{\frac{1}{3}}$ layer and that equations (2.1) represent uniformly the quasi-geostrophic dynamics all the way up to the vertical wall where the no-slip conditions are imposed on the geostrophic motion. This point is also made by Hart (1972) and it is proved by Brevdo (1983) using detailed arguments and expansions similar to those of Walker & Stewartson (1972). Thus (2.1), which are uniformly valid for $\epsilon = O(E^{\frac{1}{2}})$, can now be supplemented by the boundary conditions along the cylinder

$$\frac{\partial P_n}{\partial r} = 0, \quad \frac{\partial P_n}{\partial \theta} = 0 \quad \text{on} \quad r = 1, \tag{2.5}$$

and at infinity

$$P_n = -U_n r \sin\theta \quad \text{for } r \rightarrow \infty. \tag{2.6}$$

From the normalization it follows that

$$U_1 + U_2 = \pm 2, \tag{2.7}$$

since we shall consider on-coming flows which are either prograde or retrograde.

The results of the next Section demonstrate that quasi-geostrophic dynamics is capable of explaining the influence of β on the separation problem in prograde and retrograde flows in agreement with the observations of Boyer & Davis (1982). The left–right asymmetry with respect to the mainstream direction observed in those experiments cannot be explained, however, by the quasi-geostrophic dynamics. To explain it the non-quasi-geostrophic analysis of Merkine & Solan (1979) must be used.

3. Results and discussion

The formal derivation of (2.1) is based on the asymptotic constraint that $E_n^{\frac{1}{2}} = O(\epsilon)$ as $\epsilon \rightarrow 0$. This implies that diffusion of vorticity is of no consequence away from the vertical boundary layers along the cylinder. It follows that the solution of (2.1) can be determined by matching the solution of the diffusion-free interior to the diffusion-dominated solution that exists in the vertical boundary layer adjacent to the cylinder.

In this section we determine the solution for the following parameter regimes: $\beta = O(1)$ for $0 \leqslant E_n^{\frac{1}{2}}/\epsilon \leqslant \infty$ and $\beta\epsilon/E_n^{\frac{1}{2}} = O(1)$ for $E_n^{\frac{1}{2}}/\epsilon \gg 1$. Formally, the derivation of the equations for $E_n^{\frac{1}{2}} \gg \epsilon$ should be based on using $E_n^{\frac{1}{2}}$ rather than ϵ as the expansion parameter. Nevertheless (2.1) are uniformly valid for $0 \leqslant E_n^{\frac{1}{2}}/\epsilon \leqslant \infty$ and by rescaling the β parameter such that $\beta\epsilon/E_n^{\frac{1}{2}} = O(1)$ we can consider the case where the β-effect operates on the same dynamical level as the Ekman suction while nonlinear effects can be ignored.

3.1. $\beta = O(1)$ *and* $0 \leqslant E_n^{\frac{1}{2}}/\epsilon \leqslant \infty$

We consider first the case of $E_n^{\frac{1}{2}}/\epsilon \ll 1$ and assume that the vortex-stretching mechanism induced by the Ekman layers can be ignored. It then follows from (2.1) that potential vorticity is conserved in the interior implying that

$$\nabla^2 P_n + (-1)^n F_n(P_1 - P_2) + \beta y = Q_n(P_n) \quad (n = 1, 2). \tag{3.1}$$

In the absence of closed streamlines $Q_n(P_n)$ can be determined from the conditions at infinity, namely (2.6) and we obtain

$$Q_n(P_n) = [(-1)^n F_n(U_1 - U_2) - \beta]\, P_n/U_n \quad (n = 1, 2). \tag{3.2}$$

It is convenient to introduce the perturbation stream function

$$\psi_n = P_n + U_n y \tag{3.3}$$

whose governing equations are

$$\nabla^2\psi_n + (-1)^n F_n[\psi_1 - \psi_2 - (U_1 - U_2)\,\psi_n/U_n] + \beta\psi_n/U_n = 0 \tag{3.4}$$

and we observe† that a change in the sign of U_n is equivalent to a change in the sign of β. We adhere, however, to the standard definition of β assuming it non-negative. It follows from matching the interior solution with the boundary-layer solution that the no-penetration boundary condition can be imposed directly on the lowest-order interior motion implying that

$$\psi_n = U_n \sin\theta, \quad \text{on } r = 1. \tag{3.5}$$

The domain of integration is multiply connected and for $\beta \neq 0$ the solution is determined up to an arbitrary r-dependent circulation. We eliminate this circulation by applying the argument of Walker & Stewartson (1972). Although in the present case the Ekman suction mechanism is assumed negligible, Ekman layers do exist. An interior circulation would induce unidirectional radial mass flux in the Ekman layers which could only be maintained by a distribution of sources or sinks along the cylinder. This is not the case at hand.

The boundary-value problem governing ψ_n is completely specified when the boundary conditions at infinity are stated. The condition that the ψ_ns decay at infinity may not be enough to ensure uniqueness if stationary waves exist. When this happens we must impose the radiation condition. We restrict ourselves to flows which are either prograde or retrograde at infinity. From the dispersion relation it follows (i) that stationary Rossby waves with positive x-component group velocity exist in prograde flows, (ii) that no stationary Rossby waves exist in retrograde flows. Consequently the following conditions at infinity are imposed:

$$r^{\frac{1}{2}}\psi_n \to 0 \quad \text{upstream for prograde flows,} \tag{3.6}$$

$$\psi_n \to 0 \quad \text{as} \quad r \to \infty \text{ for retrograde flows.} \tag{3.7}$$

The two equations of (3.4) can be linearly combined to yield

$$\nabla^2(a\psi_1 + b\psi_2) = (N_1 a - F_2 b)\,\psi_1 + (N_2 b - F_1 a)\,\psi_2, \tag{3.8}$$

where a and b are arbitrary constants and

$$N_1 = \frac{(F_1 U_2 - \beta)}{U_1}, \quad N_2 = \frac{(F_2 U_1 - \beta)}{U_2}, \quad N_3 = F_1 F_2. \tag{3.9}$$

Choosing a and b as the non-trivial solutions of the homogeneous problem

$$\begin{pmatrix} N_1 & -F_2 \\ -F_1 & N_2 \end{pmatrix}\begin{pmatrix} a \\ b \end{pmatrix} = -\lambda\begin{pmatrix} a \\ b \end{pmatrix}, \tag{3.10}$$

we find that (3.8) reduces to Helmholtz's equation

$$\nabla^2\phi_n = -\lambda_n\phi_n \quad (n = 1, 2), \tag{3.11}$$

where the λ_ns are the eigenvalues of (3.10), namely

$$\lambda_{1,2} = -\tfrac{1}{2}(N_1 + N_2) \pm \tfrac{1}{2}[(N_1 - N_1)^2 + 4N_3]^{\frac{1}{2}}, \tag{3.12}$$

and

$$\phi_1 = F_2\psi_1 + (N_1 + \lambda_1)\,\psi_2, \quad \phi_2 = (N_2 + \lambda_2)\,\psi_1 + F_1\psi_2. \tag{3.13}$$

† This was pointed out by a referee.

From (3.5) and (3.13) it follows that

$$\phi_n = c_n \sin\theta \quad \text{on} \quad r = 1, \tag{3.14}$$

where
$$c_1 = F_2 U_1 + (N_1+\lambda_1) U_2, \quad c_2 = (N_2+\lambda_2) U_1 + F_1 U_2, \tag{3.15}$$

while (3.6)–(3.7) translate into

$$r^{\frac{1}{2}}\phi_n \to 0 \quad \text{upstream for } \lambda_n > 0, \tag{3.16}$$

$$\phi_n \to 0 \quad \text{as } r\to\infty \quad \text{for } \lambda_n < 0. \tag{3.17}$$

The procedure leading to the boundary-value problem for the ϕ_ns is equivalent to separating the motion into its barotropic and baroclinic components.

The boundary-value problem for ϕ_n is mathematically identical to the barotropic problem treated by Merkine (1980) for prograde and retrograde flows. For prograde flows ($\lambda_n > 0$) the solution is a direct adaptation of the solution of Miles (1968) who studied lee waves generated by stratified flow past a semi-circular obstacle. (Miles' technique was applied also by McCartney (1975) to the problem of inviscid flow over a short bump in a two-layer model on a β-plane.) The solution is

$$
\begin{aligned}
\phi_n &= \sum_{q=1}^{\infty} g_q f_q, \\
f_q &= a_q\left(Y_q(\lambda_n^{\frac{1}{2}} r)\sin q\theta + \sum_{p=1}^{\infty} b_{qp} J_p(\lambda_n^{\frac{1}{2}} r)\sin p\theta\right), \\
a_q &= -\frac{\pi(\frac{1}{2}\lambda_n^{\frac{1}{2}})^q}{(q-1)!}, \\
b_{qp} &= \frac{4}{\pi^2}\frac{q}{p^2-q^2} \quad (q \text{ even}, \quad p \text{ odd}), \\
&= \frac{4}{\pi^2}\frac{p}{p^2-q^2} \quad (q \text{ odd}, \quad p \text{ even}), \\
&= 0 \quad (q-p \text{ even}),
\end{aligned} \tag{3.18}
$$

$$\sum_{q=1}^{\infty} a_q[\delta_{pq} Y_p(\lambda_n^{\frac{1}{2}}) + b_{qp} J_p(\lambda_n^{\frac{1}{2}})] g_q = c_n \delta_{1p} \quad (p = 1, 2, \ldots).$$

The coefficients g_q are determined by solving an infinite set of linear equations. Approximate solutions are obtained by truncation. For the range of parameters considered here truncation to six equations was adequate. The results differed from the seven-equation system in the fifth significant digit.

For retrograde flows ($\lambda_n < 0$) the solution is simple. It is given by

$$\phi_n = c_n K_1(|\lambda_n|^{\frac{1}{2}} r)\sin\theta / K_1(|\lambda_n|^{\frac{1}{2}}). \tag{3.19}$$

Once the ϕ_ns are determined the perturbation streamfunctions, ψ_1 and ψ_2, follow from (3.13) and the geostrophic pressures, P_1 and P_2, from (3.3).

When the interior solution generates closed circulations, and this can occur in prograde flows, the assumption leading to (3.1), namely that $E_n^{\frac{1}{2}}/\epsilon \ll 1$ can be approximated by $E_n^{\frac{1}{2}}/\epsilon = 0$, breaks down since the potential vorticity is left undetermined in the closed circulation regions. In this case the interior flow must be determined numerically. However, when $E_n^{\frac{1}{2}}/\epsilon$ is not small the numerical approach is necessary for both prograde and retrograde flows. The method for integrating the interior equations is described in the Appendix. Once the interior solution is determined (analytically or numerically) the azimuthal velocity impressed by it on the cylinder is known and the boundary-layer equations can be solved. The method of solution of these coupled nonlinear equations is described in detail in Brevdo & Merkine (1985) for a potential flow interior. With minor modifications it can be applied to any interior flow.

The solution of the nonlinear boundary-layer equations derived from (2.1) terminates, as stated in §1, in the vicinity of θ_s where the vanishing wall shear stress signals the breakaway of the nonlinear quasi-geostrophic vertical boundary layer. This should signal, however, the separation of the entire $O(1)$ flow since the wall shear stress induced by the inner $E^{\frac{1}{3}}$ layer is $O(E^{\frac{1}{6}})$ relative to the wall shear stress induced by the $E^{\frac{1}{4}}$ layer and hence negligible in an asymptotic sense. (The tangential velocity in the $E^{\frac{1}{3}}$ layer is $O(E^{\frac{1}{4}})$, Walker & Stewartson 1972.)

Since the flow field depends on six parameters, exhausting all possibilities is impractical. Hence we restrict our presentation to $\delta_1 = \delta_2 = \delta$, $E_1 = E_2 = E$, $\chi = 1$ and $F_1 = F_2 = 1$ and for this choice of parameters the boundary-layer equations derived from (2.1) assume the form

$$\left(\bar{u}_1\frac{\partial}{\partial \xi}+\bar{v}_1\frac{\partial}{\partial \theta}\right)\bar{v}_1 = V_1\frac{\partial V_1}{\partial \theta}+\frac{E^{\frac{1}{2}}}{2^{\frac{3}{2}}\epsilon}[3(V_1-\bar{v}_1)+\bar{v}_2-V_2]+\frac{E^{\frac{1}{2}}\delta^2}{\epsilon}\frac{\partial^2\bar{v}_1}{\partial \xi^2},$$

$$\left(\bar{u}_2\frac{\partial}{\partial \xi}+\bar{v}_2\frac{\partial}{\partial \theta}\right)\bar{v}_2 = V_2\frac{\partial V_2}{\partial \theta}+\frac{E^{\frac{1}{2}}}{2^{\frac{3}{2}}\epsilon}[3(V_2-\bar{v}_2)+\bar{v}_1-V_1]+\frac{E^{\frac{1}{2}}\delta^2}{\epsilon}\frac{\partial^2\bar{v}_2}{\partial \xi^2},$$

$$\frac{\partial \bar{u}_n}{\partial \xi}+\frac{\partial \bar{v}_n}{\partial \theta} = 0,$$

$$\bar{u}_n = \bar{v}_n = 0 \quad \text{on } \xi = 0,$$

$$\bar{v}_n = V_n \quad \text{as } \xi \to \infty.$$

Here $\bar{u}_n$ and $\bar{v}_n$ are the radial and tangential velocity components in the boundary layer. V_n is the interior tangential velocity impressed on the boundary layer and $\xi = (r-1)/E^{\frac{1}{4}}$ is the boundary-layer coordinate. We note also that $\delta = O(1)$ and $E^{\frac{1}{2}}/\epsilon = O(1)$.

From all cases considered retrograde flows are the simplest since the interior solution possesses no wavy structure and it decays exponentially at large distances form the cylinder. Merkine's (1980) barotropic study showed that the interior azimuthal velocity impressed on the cylinder increases with β but since Ekman suction was negligible the increase in velocity could not affect the boundary-layer dynamics which were identical to the non-rotating case. Yet Boyer & Davies (1982) observed in their experiments that separation was enhanced in retrograde flows. Merkine's (1980) analysis was for large Reynolds numbers but the onset of separation took place at moderate Reynolds numbers. Since the interior azimuthal velocity at the cylinder increases with β this is equivalent to decreasing the effective Reynolds number (based on the velocity at infinity) necessary for triggering separation. A more likely explanation of the observations of Boyer & Davies is based on the fact that Ekman suction was not negligible in their experiments. This point is demonstrated in figure 1 depicting the angle of separation as a function of $\epsilon/E^{\frac{1}{2}}$ for $U_1 = U_2 = -1$ and several values of β denoted in the figure by β_r for retrograde flow. When $U_1 = U_2$ the response of the system is purely barotropic since the baroclinic mode vanishes. Hence this case corresponds to the experimental set-up of Boyer & Davies. We see that β enhances separation. The effect is small for large values of $\epsilon/E^{\frac{1}{2}}$ in agreement

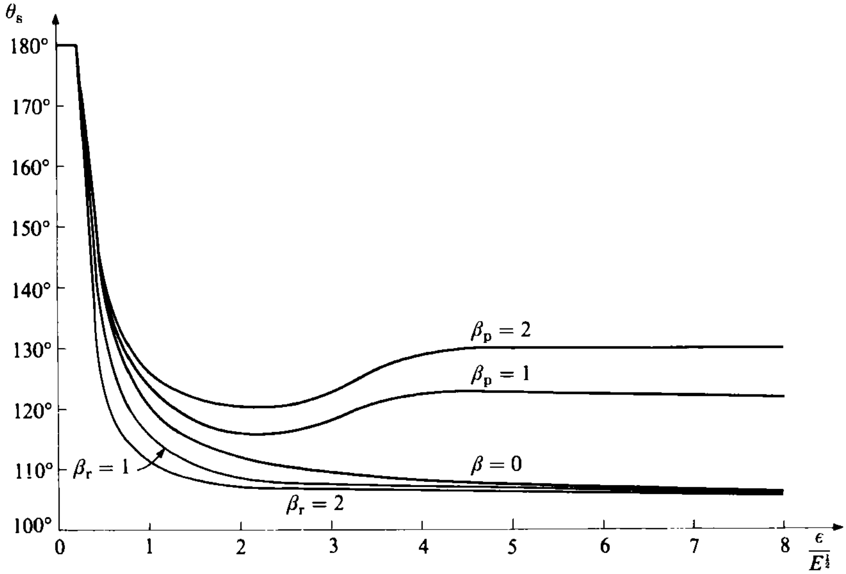

FIGURE 1. The angle of separation θ_s measured from the forward stagnation point as a function of $\epsilon/E^{\frac{1}{2}}$ for the barotropic retrograde and prograde flows $U_1 = U_2 = -1$ and $U_1 = U_2 = 1$, respectively. The values of β for retrograde and prograde flows are denoted by β_r and β_p, respectively.

with Merkine's (1980) prediction. It is significant, however, for moderate values of $\epsilon/E^{\frac{1}{2}}$. (In this case the entire flow field must be determined numerically.) The effect of Ekman suction on the interior is to dissipate the relative vorticity generated by the β-effect when fluid particles are displaced laterally. This breaks down the east–west symmetry of the inertial solution (3.19) and induces an adverse pressure gradient in the boundary layers which penetrates into the forward half (relative to the forward stagnation point) of the cylinder. Although Ekman suction also dissipates the wall vorticity the symmetry cannot be restored and separation is enhanced as figure 1 indicates. However, when $\epsilon/E^{\frac{1}{2}} \ll 1$ the interior production of relative vorticity by the β-effect is insignificant since $\beta = O(1)$ and the east–west symmetry is restored in the interior which assumes the form of a potential flow. This is reflected in figure 1 where all curves converge for $\epsilon/E^{\frac{1}{2}} \ll 1$.

The inertial ($E^{\frac{1}{2}}/\epsilon \ll 1$) interior prograde flows do not possess the east–west symmetry of the intertial retrograde flows because of the presence of stationary Rossby waves. The dependence of the angle of separation on the ratio $E^{\frac{1}{2}}/\epsilon$ for $U_1 = U_2 = 1$ and several values of β, denoted in the figure by β_p for prograde flows, is depicted also in figure 1. We point out again that since $U_1 = U_2$ this case corresponds to the barotropic experiments of Boyer & Davies (1982). In agreement with the experiments and contrary to the retrograde case discussed above we observe that β inhibits separation. For large values of $\epsilon/E^{\frac{1}{2}}$ the limiting values of the curves approach Merkine's (1980) results asymptotically. When $\epsilon/E^{\frac{1}{2}} \ll 1$ and since $\beta = O(1)$ the interior relative vorticity production induced by the β-effect is rapidly destroyed, the dependence on β is lost and all curves converge to the f-plane case. Figure 1 indicates also that for $\beta \neq 0$ the dependence of the separation angle on $\epsilon/E^{\frac{1}{2}}$ is not monotonic for prograde flows. In particular, for moderate values of $\epsilon/E^{\frac{1}{2}}$ separation occurs earlier than when Ekman suction is negligible. To understand this phenomenon we recall

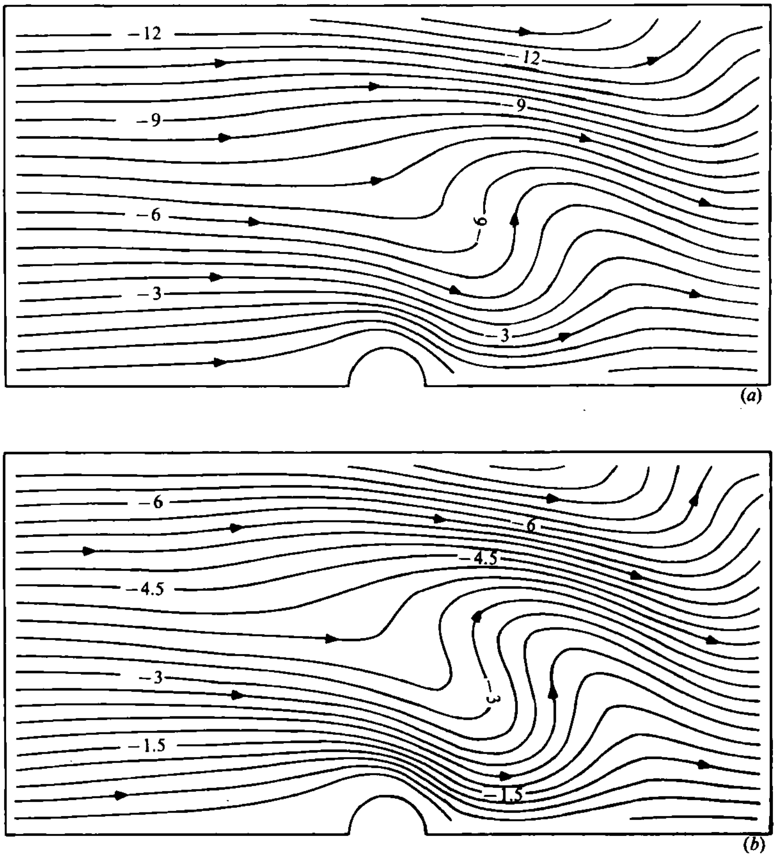

FIGURE 2. Streamlines of the interior intertial ($E^{\frac{1}{2}}/\epsilon = 0$) prograde flow for $U_1 = 1.3$, $U_2 = 0.7$ and $\beta = 1$. (*a*) Upper layer; (*b*) lower layer.

first (Merkine 1980) that the strong east–west asymmetry of the interior inertial prograde regime inhibits separation by pushing toward the rear stagnation point the adverse pressure gradient impressed on the cylinder. In the presence of Ekman suction interior relative vorticity is destroyed and the east–west asymmetry weakens. (An opposite effect takes place in retrograde flows.) Consequently the adverse pressure gradient is pushed backwards towards the forward stagnation point. For $\epsilon/E^{\frac{1}{2}} \gtrsim 1$ this effect is stronger than the separation-inhibiting effect played by the Ekman suction in the boundary-layer dynamics and separation is accelerated.

Shifting our attention to baroclinic flows we depict in figure 2 a typical inviscid, prograde, interior flow. As a general rule the amplitude of the stationary Rossby wave field is more pronounced in the slower, lower layer and in both layers it increases with β. Closed circulations appear first in the lower layer, invalidating the assumptions leading to the inertial solution, namely that the potential vorticity distribution can be determined everywhere by tracing the particles' paths to infinity. When this happens we have a problem of singular perturbation. The $E^{\frac{1}{2}}/\epsilon \ll 1$ dynamics cannot be approximated to lowest order by the $E^{\frac{1}{2}}/\epsilon = 0$ dynamics and as in barotropic cases, the interior dynamical equations must be integrated numerically. The interior, baroclinic, inertial solution for retrograde flow derived from (3.19) is extremely simple and requires no graphical presentation.

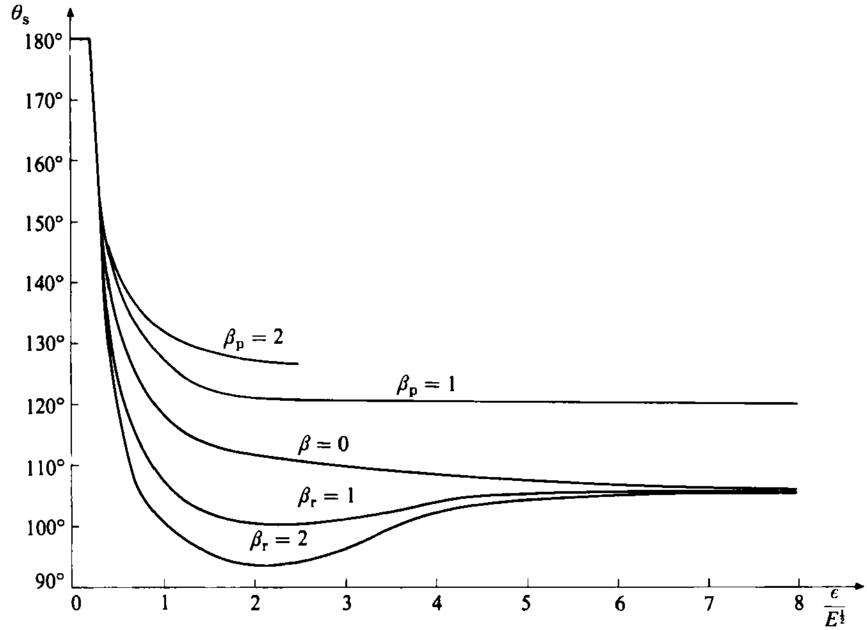

FIGURE 3. The same as in figure 1 but for the baroclinic retrograde and prograde flows $U_1 = -1.6$, $U_2 = -0.4$ and $U_1 = 1.6$, $U_2 = 0.4$, respectively.

Figure 1 indicates that the angle of separation is a monotonic function of $\epsilon/E^{\frac{1}{2}}$ for retrograde flows and non-monotonic for prograde flows. The trend is opposite when the flow at infinity is vertically sheared as figure 3 shows. For retrograde flows, $U_1 = -1.6$, $U_2 = -0.4$ and $\beta = \beta_r$ the small lower-layer velocity increases the local effect of β in the relative vorticity production by allowing greater lateral displacement of fluid particles. This enhances the interior east–west asymmetry created by Ekman suction to the extent that for moderate values of $\epsilon/E^{\frac{1}{2}}$ separation occurs at angles which are closer to the forward stagnation point than in the inertially dominated case $\epsilon/E^{\frac{1}{2}} \gg 1$. Our results indicate that regardless of U_1 and U_2 the separation angle in retrograde flows seems to be the same in both layers.

For the prograde flows, $U_1 = 1.6, U_2 = 0.4$ and $\beta = \beta_p$ the smaller lower-layer velocity enhances again the β-effect and hence the separation-inhibiting effect of the interior east–west asymmetry. Thus stronger Ekman suction is necessary to remove the east–west asymmetry in the interior. But this process which tends to accelerate separation is counteracted now more easily by the stronger Ekman suction in the boundary layer and separation is inhibited.

Our results indicate that for vertically sheared prograde flows the decrease in the wall shear stress on the approach to separation is more rapid in the upper layer than in the lower layer. However, on account of the singular behaviour of the boundary-layer equations in the vicinity of the point of separation no definite conclusion could be drawn as to whether separation indeed occurred earlier in the upper layer.

The results of Brevdo & Merkine (1985) for the two-layer f-plane separation problem show that for sufficiently strong vertical shear, a backflow inner region can exist in the boundary layer of the lower layer without separation taking place. This can also occur on a β-plane but in view of the extensive discussion given to this phenomenon in Brevdo & Merkine (1985) we will not pursue it here any further.

3.2. $\beta\epsilon/E_n^{\frac{1}{2}} = O(1)$, $E_n^{\frac{1}{2}}/\epsilon \gg 1$

In this parameter regime the contributions of the relative vorticity and the displacement of the interface to the potential vorticity are negligible and equations (2.1) reduce in the interior to

$$\left.\begin{aligned} B_1\frac{\partial P_1}{\partial x} &= -\nabla^2 P_1 + \frac{\chi}{\chi+1}(\nabla^2 P_2 - \nabla^2 P_1), \\ B_2\frac{\partial P_2}{\partial x} &= -\nabla^2 P_2 + \frac{1}{\chi+1}(\nabla^2 P_1 - \nabla^2 P_2), \end{aligned}\right\} \tag{3.20}$$

where $B_n = \beta\epsilon/E_n^{\frac{1}{2}} = O(1)$. These equations can be linearly combined to yield

$$\frac{\partial}{\partial x}(aP_1 + bP_2) = \nabla^2[(A_{11}a + A_{21}b)P_1 + (A_{12}a + A_{22}b)P_2],$$

where a and b are arbitrary constants and

$$\left.\begin{aligned} A_{11} &= -\frac{2\chi+1}{(\chi+1)B_1}, \quad A_{12} = \frac{\chi}{(\chi+1)B_1}, \\ A_{21} &= \frac{1}{(\chi+1)B_2}, \quad A_{22} = -\frac{\chi+2}{(\chi+1)B_2}. \end{aligned}\right\} \tag{3.21}$$

Defining the perturbation streamfunctions

$$\psi_n = P_n + U_n y, \tag{3.22}$$

and choosing a and b as the non-trivial solutions of the homogeneous problem

$$\begin{pmatrix} A_{11} & A_{21} \\ A_{12} & A_{22} \end{pmatrix}\begin{pmatrix} a \\ b \end{pmatrix} = \lambda\begin{pmatrix} a \\ b \end{pmatrix} \tag{3.23}$$

(3.20) reduces to the two equations

$$\nabla^2\phi_n = \frac{1}{\lambda_n}\frac{\partial\phi_n}{\partial x} \quad (n = 1, 2), \tag{3.24}$$

governing the barotropic and baroclinic modes of the flow fields where the λ_ns are the eigenvalues of (3.23), namely,

$$\lambda_{1,2} = \tfrac{1}{2}(A_{11} + A_{22}) \pm \tfrac{1}{2}[(A_{11} - A_{22})^2 + 4A_{12}A_{21}]^{\frac{1}{2}}, \tag{3.25}$$

and

$$\phi_n = \psi_1 + \frac{A_{12}}{\lambda_n - A_{22}}\psi_2 \quad (n = 1, 2). \tag{3.26}$$

From (3.21) and (3.25) it follows that $\lambda_{1,2} < 0$. Consequently the boundary conditions imposed on the ψ_ns are (3.5) and (3.7) which translate into

$$\left.\begin{aligned} &\phi_n = C_n \sin\theta \quad \text{on} \quad r = 1, \\ &C_n = U_1 + \frac{A_{12}}{\lambda_n - U_{22}}U_2 \quad (\phi_n \to 0 \quad \text{as} \quad r \to \infty). \end{aligned}\right\} \tag{3.27}$$

The transformation

$$\phi_n = G_n \exp\left(\frac{x}{2\lambda_n}\right), \tag{3.28}$$

eliminates the first derivative from (3.24) and we find that G_n is governed by Helmholtz's equation

$$\nabla^2 G_n = \frac{1}{4\lambda_n^2} G_n, \tag{3.29}$$

subject to the boundary conditions

$$G_n = C_n \sin\theta \exp\left(\frac{-\cos\theta}{2\lambda_n}\right) \quad \text{on} \quad r = 1, \tag{3.30}$$

$$G_n = o\left(\exp\left(\frac{x}{2\lambda_n}\right)\right) \quad \text{as} \quad r \to \infty. \tag{3.31}$$

It is straightforward to show that

$$\left.\begin{aligned} G_n &= C_n \sum_{m=1}^{\infty} b_m K_m\left(\frac{r}{2|\lambda_n|}\right) \sin m\theta, \\ b_m &= \frac{1}{\pi K_m(1/2|\lambda_n|)} \int_0^{2\pi} \sin\theta \exp\left(\frac{\cos\theta}{2|\lambda_n|}\right) \sin m\theta \, \mathrm{d}\theta \\ &= 4|\lambda_n| m\, I_m\left(\frac{1}{2|\lambda_n|}\right) \Big/ K_m\left(\frac{1}{2|\lambda_n|}\right). \end{aligned}\right\} \tag{3.32}$$

The integral in the expression for b_m was evaluated by differentiating with respect to θ the identity

$$\exp(z\cos\theta) = I_0(z) + 2\sum_{j=1}^{\infty} I_j(z) \cos j\theta. \tag{3.33}$$

(Abramowitz & Stegun 1970).

The solution for ϕ_n is obtained by substituting (3.32) into (3.28). With the ϕ_ns determined, the P_ns follow from (3.26) and (3.22). The east–west asymmetry discussed in the previous section exists also in the present case as can be inferred from (3.20). We observe also that since the eigenvalues (3.25) are independent of the velocity at infinity (on account of the strong damping no stationary Rossby waves can exist) the same streamline pattern is obtained for prograde and retrograde flows. The only difference is that the flow direction is reversed. The asymmetry is introduced by the Ekman suction mechanism which organizes the attributes of the vorticity field in the eastern sector, $|\theta| < \frac{1}{2}\pi$, in a different manner from those in the western sector, $\frac{1}{2}\pi < |\theta| < \pi$, independent of the flow direction at infinity. To see this it suffices to consider the barotropic case. We note that in the vicinity of the cylinder the interior radial velocity is weak and the streamlines are nearly circular. Thus, in the immediate vicinity of the cylinder the attributes of the vorticity field are the shear of the azimuthal velocity and the curvature effect of the streamlines, namely $\partial v/\partial r$ and v/r, respectively. There two must combine to offset the creation of vorticity by the meridional displacement of the fluid particles on the β-plane. Let us consider, for example, retrograde flows and the range $0 < \theta < \pi$. In the eastern sector particles are displaced northward and the vorticity must be negative. The curvature vorticity is positive, however. This implies that the shear vorticity must be negative and sufficiently strong to counteract the combined effect of curvature and β. It follows that streamlines must converge and that a jet should form in the eastern sector. In the western sector particles are displaced southward and the vorticity must be positive. The curvature vorticity is still positive and it cancels partially the contribution of the β-effect. It follows that the shear vorticity need not be strong and this can lead to the divergence of streamlines. Thus, the streamline pattern possesses east–west asymmetry and this effect increases with β. We can apply the same reasoning to prograde flows but the end result is the same. A jet is formed in the eastern sector and streamlines diverge in the western sector.

These features can be illustrated easily in the limit of a large β-effect. We consider for simplicity the case of $\chi = 1$ and $B_1 = B_2 = B$. From (3.25) it follows that $\lambda_1 = -1/B$, $\lambda_2 = -2/B$ where λ_1 and λ_2 correspond to the barotropic and baroclinic modes, respectively. For $2|\lambda_n| \ll 1$ we can use the asymptotic properties of modified Bessel K-functions for large arguments and expression (3.33) to derive the following approximate expression for the solution:

$$\left.\begin{aligned} P_1 \simeq -U_1 r\sin\theta + \sin\theta\{(U_1+U_2)\exp[-B(r-1)(1+\cos\theta)/2] \\ +(U_1-U_2)\exp[-B(r-1)(1+\cos\theta)/4]\}/2r^{\frac{1}{2}}, \\ P_2 \simeq -U_2 r\sin\theta + \sin\theta\{(U_1+U_2)\exp[-B(r-1)(1+\cos\theta)/2] \\ -(U_1-U_2)\exp[-B(r-1)(1+\cos\theta)/4]\}/2r^{\frac{1}{2}}, \end{aligned}\right\} \tag{3.34}$$

where $U_1 + U_2 = \pm 2$. The plus sign is for prograde flows; the minus sign is for retrograde flows.† When $U_1 = U_2 = \pm 1$ the response is pure barotropic and (3.34) simplifies to

$$P_1 = P_2 \simeq \pm\sin\theta\{-r + r^{-\frac{1}{2}}\exp[-B(r-1)(1+\cos\theta)/2]\}. \tag{3.35}$$

The azimuthal velocity is given by

$$v_1 = v_2 \simeq \pm\sin\theta\left\{1 + \frac{1}{2r^{\frac{1}{2}}}\left(\frac{1}{r} + B(1+\cos\theta)\right)\exp[-B(r-1)(1+\cos\theta)/2]\right\}, \tag{3.36}$$

which reduces on the cylinder to the following expression

$$v_1 = v_2 \simeq \mp\sin\theta\{1 + \tfrac{1}{2}[1 + B(1+\cos\theta)]\}. \tag{3.37}$$

For large B the jet is strongest at

$$\cos\theta \simeq \frac{1}{2}\left(1 - \frac{1}{B}\right) \quad \text{or} \quad |\theta| \sim \tfrac{1}{3}\pi + \frac{1}{3^{\frac{1}{2}}B}. \tag{3.38}$$

From (3.35) it follows that the width of the jet in the eastern sector is inversely proportional to B, much the same as in Stommel's (1948) Gulf stream model. We note, however, that for such an approximation to have any validity we must require that the width of the jet be much larger than the $E^{\frac{1}{4}}$ layer or that $\beta\epsilon \ll E^{\frac{1}{4}}$. In the western sector the boundary layer widens appreciably since $1 + \cos\theta$ decreases and in the parabolic sector $(r-1)(\theta-\pi)^2 \ll 4/B$ the decay is algebraic. These features can be observed in figure 5(*c*) of Boyer & Davies (1982). When the constraint $B \gg 2$ is not satisfied the exact solution must be used. Figure 4 depicts such a case for $\beta = \sqrt{2}/2$ and a weak east–west asymmetry is observed.

When the flow is baroclinic (3.34) can be used when $B \gg 4$. The decay rate of the baroclinic mode is half as strong as that of the barotropic mode and the latter can

† Equation (3.34) is not an asymptotic representation of the exact solution for large B since the asymptotic representation of Bessel functions for large arguments is not uniformly valid for large orders. Nevertheless, comparison of (3.34) with the exact solution shows that it is qualitatively correct.

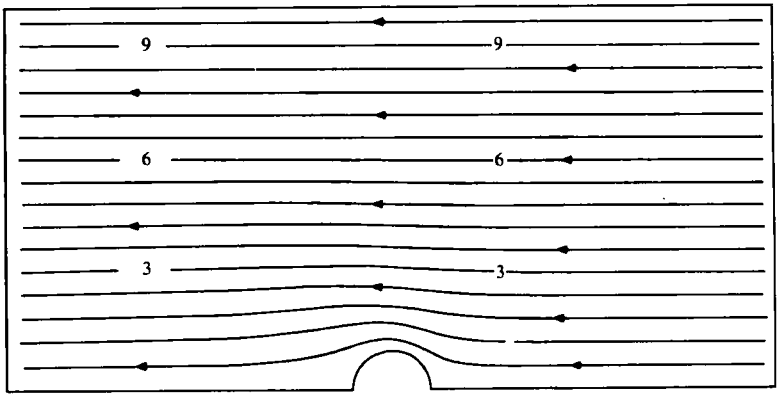

FIGURE 4. Streamlines of the interior linear solution governed by (3.20) for the barotropic retrograde flow $U_1 = U_2 = -1$, $B_1 = B_2 = 2^{-\frac{1}{2}}$ and $\chi = 1$. The solution for barotropic prograde flow is obtained by reversing the direction of the arrows leaving everything else unchanged.

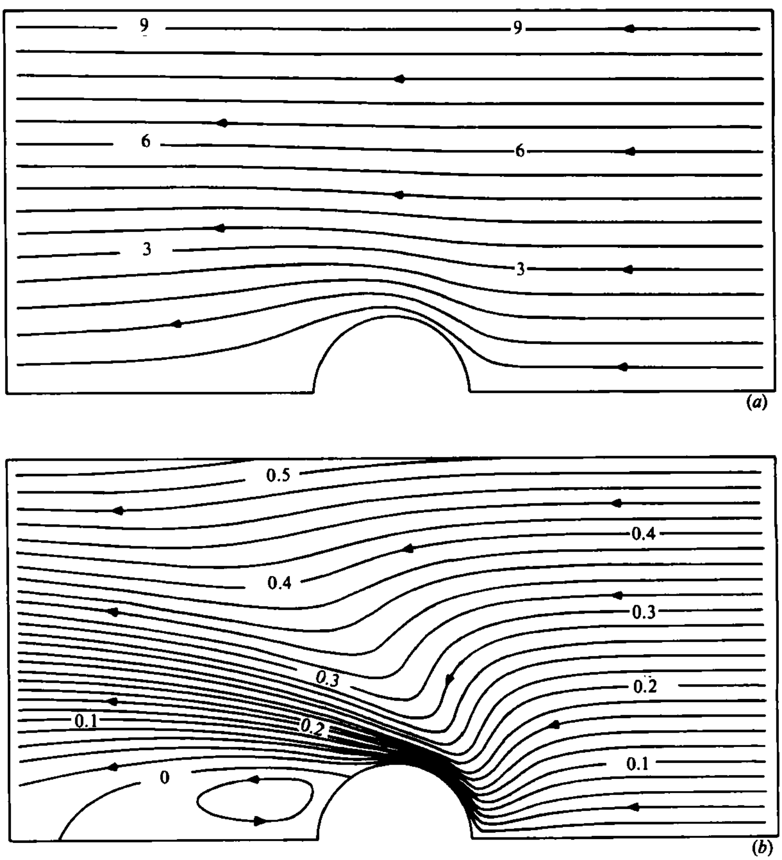

FIGURE 5. The same as in figure 4 but for the baroclinic flow $U_1 = -1.9$, $U_2 = -0.1$ and $\beta = 2^{\frac{1}{2}}$. To obtain the corresponding prograde solution reverse the directions of the arrows leaving everything else unchanged. (a) Upper layer; (b) lower layer.

be ignored at large distances from the cylinder. However, at such distances the response is exponentially small. Hence, in order to appreciate the role of baroclinicity we must require that U_2 be small. To emphasize, we set $U_2 = 0$ and (3.34) yields the following expression for the lower-layer flow

$$P_2 \simeq \pm \sin\theta\{\exp[-B(r-1)(1+\cos\theta)/2] - \exp[-B(r-1)(1+\cos\theta)/4]\}/r^{\frac{1}{2}}. \quad (3.39)$$

We see that P_2 vanishes on $r = 1$ and as $r \to \infty$, and consequently it is not monotonic. It follows that the azimuthal velocity changes its direction. In the baroclinically dominated domain, i.e. when the magnitude of P_2 decreases with r the azimuthal velocity is in the opposite direction to the upper-layer main-flow direction.

This phenomenon can be understood if we note first that the interface can be considered as a source of vorticity which is equal to the average vorticity, i.e. to the vorticity of the barotropic mode. Hence, the action of the interface on a given layer is to spin it up proportionally to the vorticity difference existing between the interface and the layer. When the motion is barotropic or potential the action of the interface disappears. However, when the motion is baroclinic and not potential the interface acts in a way which reinforces the motion in the mainstream direction of the upper layer and counteracts it in the lower layer. It is the combination of relative vorticity production and baroclinicity which can generate regions of backflow. In the interior, relative vorticity is generated by the β-effect. In the vertical boundary layers it is generated by the action of the walls. Although the azimuthal velocity derived from (3.39) is intense, being $O(B)$ for $1+\cos\theta > 0$, it is confined to a region of $O(B^{-1})$ next to the wall. When B decreases, the azimuthal velocity also decreases with a larger portion of the flow field disturbed. For moderate values of B the exact solution must be used and an example is shown in figure 5 for $U_1 = 1.9$, $U_2 = 0.1$ and $B = 2^{\frac{3}{2}}$. All the features discussed above can be seen. The most striking feature is the large horizontal extent of the closed eddy, which although weak does not spin-down to a state of rest because of the action of the interface discussed above.

The lowest-order solution described in this section is completed by adjusting the interior azimuthal velocity impressed on the cylinder to the no-slip wall condition through a linear $E^{\frac{1}{4}}$ vertical Stewartson layer which depends parametrically on θ. For sufficiently strong vertical shear this layer can develop locally an inner backflow region as shown by Brevdo & Merkine (1985).

This paper is partly based on the doctoral thesis of L. Brevdo submitted to the Technion's Graduate School under the supervision of Professor L. Merkine.

Appendix

The numerical method used for integrating the interior equations derived from (2.1)–(2.6) by neglecting the diffusion of vorticity in the interior and dropping the first condition of (2.5) is a straightforward adaptation to the two-layer model of the scheme used by Vaziri & Boyer (1971). It was convenient to use a polar grid and because of the symmetry of the equations and the boundary conditions with respect to the flow direction at infinity only half of the domain $0 \leqslant \theta \leqslant \pi$ was used. The grid interval was uniform in r and θ and equal to $\frac{1}{30}\pi$. In the radial direction the domain of integration extended to $r \simeq 12$. The equations were solved for the perturbation streamfunctions ψ_n, i.e. the deviation of the pressure from its distribution at infinity. At the upstream boundary of the domain the perturbation potential vorticity was set equal to zero. At the downstream boundary of the domain it was extrapolated linearly outwards. The initial guess for the flow field was a potential flow configuration. The streamfunctions were determined from the updated potential vorticity by solving two coupled non-homogeneous Helmholtz's problems. Convergence was achieved in about 10 iterations. The accuracy of the solution was checked by comparing the azimuthal velocity impressed on the cylinder for $U_1 = 1.3$, $U_2 = 0.7$, $\beta = 1$, $F_1 = F_2 = 1$ and $E_n^{\frac{1}{2}}/\epsilon = 0.01$ with Miles inertial solution. The comparison was satisfactory.

REFERENCES

ABRAMOWITZ, M. & STEGUN, I. A. 1970 *Handbook of Mathematical Functions*, Dover.

BARCILON, V. 1970 *Phys. Fluids* **13**, 537–544.

BOYER, D. L. 1970 *Trans. ASME* D: *J. Basic Engng* **92**, 430–436.

BOYER, D. L. & DAVIES, P. A. 1982 *Phil. Trans. R. Soc. Lond.* A **306**, 533–556.

BREVDO, L. 1983 Separation of boundary layers in a two strata flow in a rotating fluid. Ph.D. thesis, Technion – Israel Institute of Technology, Haifa.

BREVDO, L. & MERKINE, L. 1985 *Proc. R. Soc. Lond.* A **400**, 75–95.

GOLDSTEIN, S. 1948 *Q. J. Mech. Appl. Maths.* **1**, 43–69.

GREENSPAN, H. P. 1968 *The Theory of Rotating Fluids*. Cambridge University Press.

HART, J. E. 1972 *Geophys. Fluid Dyn.* **3**, 181–209.

HOGG, N. G. 1972 *Geophys. Fluid Dyn.* **4**, 51–81.

HOGG, N. G. 1980 In *Orographic Effects in Planetary Flows* (ed. R. Hide & P. H. White), pp. 167–205 G.A.R.P. Publication Series, No. 23 Geneva: World Meteorological Organization.

MCCARTNEY, M. S. 1975 *J. Fluid Mech.* **68**, 71–95.

MERKINE, L. 1980 *J. Fluid Mech.* **99**, 399–409.

MERKINE, L. 1985 *J. Fluid Mech.* **157**, 501–518.

MERKINE, L. & SOLAN, A. 1979 *J. Fluid Mech.* **92**, 381–392.

MILES, J. W. 1968 *J. Fluid Mech.* **33**, 803–814.

PAGE, M. A. 1982 *J. Fluid Mech.* **123**, 303–313.

PEDLOSKY, J. 1979 *Geophysical Fluid Dynamics*. Springer.

ROSENHEAD, L. 1963 *Laminar Boundary Layers*. Oxford University Press.

SMITH, F. T. 1982 *IMA J. Appl. Maths.* **28**, 207–281.

STOMMEL, H. 1948 *Trans. Am. Geophys. Union* **99**, 202–206.

VAZIRI, A. & BOYER, D. L. 1971 *J. Fluid Mech.* **50**, 79–95.

WALKER, J. D. & STEWARTSON, K. 1972 *Z. angew Math. Phys.* **23**, 745–752.

WHITE, W. B. 1971 *J. Phys. Oceanogr.* **1**, 161–168.